PAPER

Magnetic glyconanoparticles for selective lectin separation and purification†

Yavuz Oz, [ID] [a] Yamin Abdouni,[b] Gokhan Yilmaz,[b] C. Remzi Becer [ID] *[b,c] and Amitav Sanyal [ID] *[a,d]

A modular platform for the separation and purification of lectins using polymer coated iron oxide nanoparticles is developed. Supramolecular host–guest interactions based on an adamantane beta-cyclodextrin (β-CD) dyad are utilized to modify the polymeric interface. Poly(ethylene glycol) based hydrophilic polymer-coated magnetic iron oxide nanoparticles are fabricated using reversible addition–fragmentation chain transfer polymerization, followed by their chain-end modification to install adamantane groups on the nanoparticle surface. These adamantyl containing nanoparticles could be surface modified using β-CDs appended with appropriate ligands for intended applications. In this study, we exploit this supramolecular system for the purpose of separation and purification of lectins. Therefore, a polymer-coated magnetic nanoparticle interface was decorated with two types of mannose-containing β-CD constructs, a monodisperse heptamannose conjugated CD and a CD-based 7-arm star shaped glycopolymer for selective binding towards the concanavalin A (ConA) lectin. The monodisperse and polydisperse CD derivatives were compared in terms of their efficiency for binding to ConA. It was demonstrated that the polymeric CD construct significantly improved the binding of magnetic nanoparticles and provided an effective system for the separation and purification of ConA from a mixture of ConA and peanut agglutinin (PNA). Moreover, the surface bound isolated protein could be simply regenerated by the addition of competitive ligands such as mannose. Specificity to bind a particular lectin can be tailored by choosing the appropriate sugar based ligand, as demonstrated by the specific capture of PNA using a galactose-containing polymer. The modular nature of functionalization of the nanoparticle interface that is tunable by host–guest chemistry affords a universal system that can be easily tailored for the purification of specific proteins from mixtures.

[a]*Department of Chemistry, Bogazici University, Bebek, 34342 Istanbul, Turkey.*
E-mail: Amitav.Sanyal@boun.edu.tr
[b]*Polymer Chemistry Laboratory, School of Engineering and Materials Science, Queen Mary University of London, E1 4NS London, UK. E-mail: Remzi.Becer@warwick.ac.uk*
[c]*Department of Chemistry, University of Warwick, CV4 7AL Coventry, UK*
[d]*Center for Life Sciences and Technologies, Bogazici University, Istanbul, Turkey*
†Electronic supplementary information (ESI) available: Synthetic procedures, NMR, UV, and DLS measurements. See DOI: 10.1039/c8py01748d

Introduction

Lectins are carbohydrate binding proteins that can specifically and reversibly bind specific carbohydrates without any chemical transformations and play the role of reading the sugar code in biology.[1,2] Due to the nature of their selective and specific interaction, the lectin–carbohydrate interactions play a vital role in the development of diagnostics and therapy platforms. In general, lectins are mainly obtained from plants and are mostly purified using relevant carbohydrate conjugated affinity chromatography or membrane sorbents that only capture relevant lectins from a mixture. Even though conventional affinity chromatography is widely utilized for lectin separation,[3–5] especially for tight-binding lectins, it requires multiple washing steps resulting in a loss of weak-affinity lectins and a decrease in the purification yield. Therefore, the fabrication of an effective and facile system for lectin separation with a high purity and recovery yield has been sought by researchers. This separation system should have: (i) a high carbohydrate density to accumulate even weak-binding lectins, (ii) good stability in aqueous media and (iii) a high selectivity toward desired lectins preventing unspecific binding.

Recently, magnetic nanoparticles (MNPs) have been exploited for biomedical applications, such as drug delivery, MRI contrast agent, hyperthermia, *etc*, because of their biocompatibility and chemical and physical stability under physiological conditions.[6–9] In addition, these nanoparticles have been utilized for the magnetic separation of biomarkers and biomolecules (lectins, proteins, *etc*.)[10–14] which is a powerful alternative to conventional separation techniques because they have a very high surface area to volume ratio and the surface of

nanoparticles can be easily tuned with specific carbohydrates for selective lectin separation. These MNPs are often coated with hydrophilic and biocompatible materials such as silicon oxide and polymers to endow MNPs with good water dispersibility.[15–18] Beyond water dispersibility, a polymeric coating on the nanoparticle surface allows one to modify the surface according to the desired application.[19]

In our previous work, we reported a modular approach for the surface functionalization of nanoparticles *via* the modification of polymer chain ends originating from RAFT polymerization with modified azo-based compounds.[20] This approach allows the facile installation of a desired functional group to the polymer chain end. While any desired end group can be installed, we envisioned that a modular construct can be obtained by installation of an end group that is amenable for modification through host–guest chemistry. An adamantane based end group offers an attractive choice since it can readily undergo non-covalent host–guest inclusion complex formation with β-cyclodextrins (β-CDs).[21–27] Seminal contribution in this area was very recently reported by Ravoo and Samanta, where they investigated β-CD capped MNPs to separate a desired lectin from a lectin mixture in a magnetic field utilizing a supramolecular system.[12] MNPs were decorated with specific carbohydrates, namely mannose and galactose, exploiting an inclusion complex with adamantane carbohydrate conjugates and β-CD capped MNPs. Lectin separation from a mixture was successfully demonstrated by using two orthogonal supramolecular interactions which are adamantane/β-CD and carbohydrate/lectin. In order to suppress the non-specific interaction of the nanoparticle surface with the protein, an ethylene glycol repeat unit containing the adamantane ligand was also added to the CD-coated nanoparticle surface. A nanoparticle based system possessing an inherently protein repellant coating would be an attractive construct. Furthermore, these interactions between carbohydrates and lectins can be considerably enhanced by multivalent carbohydrate ligands. Along similar lines, a multivalent sugar β-CD derivative for the fabrication of MNPs with desired biofunctionality was recently reported by Chen and coworkers, while our work was in progress but they have not studied the selective separation of lectins.[11] They synthesized adamantane functionalized core–shell structured magnetic composite nanoparticles (MNP@SiO$_2$-Ada) and β-CD derivatives were incorporated onto these MNPs *via* host–guest interactions. A β-CD derivative conjugated with seven mannose units (CD-M) was evaluated for ConA binding capacity. They reported that multivalent mannose containing MNPs showed higher binding capacity compared to pristine particles, but particles also showed non-specific binding to some extent. It is well known that the interactions between sugars and target lectins can be dramatically increased by using multivalent glycopolymers where sugar units are in close proximity to each other resulting in a cluster glycoside effect. Along these lines, work reported to date consists of sugar unit containing polymeric brushes grafted-from MNP surfaces.[28–30] We envisioned that as an attractive alternative, a 'plug and play' type modular platform based on host–
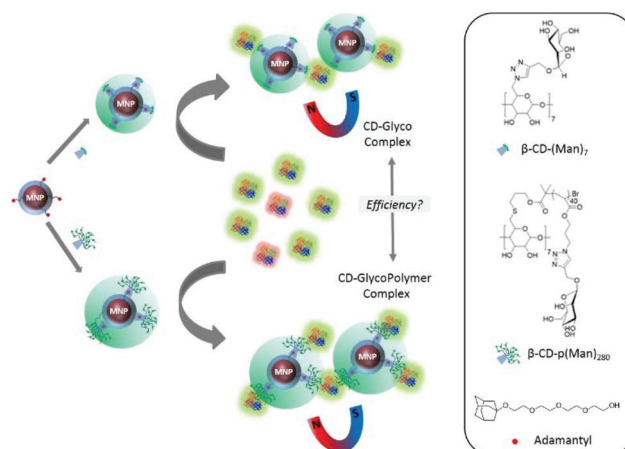
Fig. 1 Incorporation of β-CD-sugar derivatives to MNPs *via* supramolecular host–guest interactions and representation of lectin binding with these MNPs.

guest chemistry can be used to obtain sugar containing MNPs for lectin isolation and purification.

In this work, we evaluated supramolecular host–guest interactions between surface adamantane modified MNPs coated with poly(ethylene glycol) methyl ether acrylate polymers (PEGMEA) and β-CD-sugar conjugates for the separation of lectins. The surface of MNPs was modified with adamantane *via* a radical cross-coupling reaction in the presence of an adamantane modified azo-initiator. The incorporation of two β-CD-sugar conjugates to MNPs, which are β-CD conjugated with hepta-mannose (β-CD-(Man)$_7$) and conjugated with poly(mannose) (β-CD-p(Man)$_{280}$) was achieved *via* supramolecular interactions. Lectin binding efficiencies of these MNPs were evaluated in the presence of ConA. Furthermore, lectin separation from a mixture was shown using β-CD-p(Man)$_{280}$ incorporated MNPs (Fig. 1). Also, by using a galactose-containing polymer, it is demonstrated that PNA can be specifically targeted. So the system is highly modular and specific lectins can be captured by appropriate choice of glycopolymer.

Experimental

Materials

Iron(III) chloride hexahydrate (FeCl$_3$·6H$_2$O), dopamine hydrochloride, oleic acid, Aliquat® 336, 1-dodecanethiol, 4-(dimethylamino) pyridine (DMAP), tetraethylene glycol, 1-bromoadamantane, calcium chloride (CaCl$_2$), manganese chloride (MnCl$_2$) and triethylamine (TEA) were purchased from Sigma-Aldrich and used without further purification. Concanavalin A (FITC conjugate) was purchased from ThermoFisher. Poly(ethylene glycol) methyl ether acrylate (PEGMEA, M_n = 480 g mol^{-1}) was purchased from Sigma-Aldrich and purified over neutral aluminum oxide before use. 2,2′-Azobis(2-methylpropionitrile) (AIBN, Sigma) was recrystallized from methanol and dried at room temperature under vacuum prior to use.

4,4′-Azobis(4-cyanovaleric acid) (V-501) and carbon disulfide (CS$_2$) were purchased from Fluka. 1-Octadecene, N-hydroxysuccinimide (NHS), beta-cyclodextrin (β-CD) and D-(+)-mannose were purchased from Alfa-Aesar. Sodium oleate was purchased from TCI. Thin layer chromatography was performed using silica gel plates (Kieselgel 60 F254, 0.2 mm, Merck). Column chromatography was performed using silica gel 60 (43–60 nm, Merck). 2-(dodecylthiocarbonothioylthio)-2-methyl propionic acid (DDMAT),[31] DDMAT succinimide ester (DDMAT-NHS),[32] 2-(2-{2-[2-(adamantan-1-ylmethoxy)-ethoxy]-ethoxy}-ethoxy)-ethanol (Ada-TEG),[33] iron oxide nano-particles,[34] dopamine functionalized chain transfer agent (Dopa-CTA), Dopa-CTA immobilized MNPs (Fe$_3$O$_4$@CTA), polymer coated MNPs (Fe$_3$O$_4$@PEG)[20] and mannose acrylate[35] were synthesized according to previous literature examples. Dichloromethane (DCM), chloroform, ethanol, dimethyl-formamide (DMF), tetrahydrofuran (THF) and n-hexane were purchased from Merck. Anhydrous THF and DCM were obtained from the SciMatCo purification system, and other solvents were dried over molecular sieves. All other reagents and solvents were obtained at the highest purity available from Sigma Aldrich Chemical Company (Dorset, UK) and used as received unless stated otherwise. A dialysis tube (1 and 3.5 kDa MWCO) was purchased from Spectrum Laboratories (California, USA).

Instrumentation

Dynamic light scattering (DLS) and ζ-potential measurements were performed using a Malvern Zetasizer Nano ZS analyzer. Transmission electron microscopy (TEM) observations were carried out on a LVEM5 microscope operated at 5 kV. Fourier transform infrared spectroscopy (FT-IR) analyses were performed on Thermo Fisher Scientific Inc.; Nicolet 380. ^{1}H NMR and ^{13}C NMR spectra were recorded using a Bruker 400 MHz spectrometer. UV–vis studies were performed using a Varian Cary 100 Scan UV–vis spectrophotometer and a PerkinElmer UV/Vis Spectrometer Lambda 35. Fluorescence spectra were recorded on a Varian Cary Eclipse spectrophotometer (Varian, Agilent, USA). The MALDI-TOF MS spectrum acquisitions were conducted on a Shimadzu AXIMA Performance Instrument (Shimadzu Biotech, Manchester, U.K.) equipped with a 337 nm N$_2$-laser, calibrated using TOF-mixed from Laser BioLabs (Sophia-Antipolis Cedex, France). All spectra were recorded in the positive ion reflection mode. Sinapic acid (10 mg mL^{-1}) solution in acetonitrile/water (1 : 1 v/v) with 0.1% TFA was used as the matrix. The obtain spectra were analyzed using MALDI-MS software (Shimadzu Biotech, Manchester, U.K.). Size-exclusion chromatography (SEC) measurements were conducted on an Agilent 1260 infinity system operating in DMF with 5.0 mM NH$_4$BF$_4$ and equipped with a refractive index detector (RID) and variable wavelength detector (VWD), 2PLgel 5 μm mixed-C columns (300 × 7.5 mm), a PLgel 5 mm guard column (50 × 7.5 mm) and an autosampler. The instrument was calibrated with linear narrow poly(styrene) standards in range of 575 to 281 700 g mol^{-1}. All samples were passed through 0.2 μm PTFE filter before analysis. Thermal gravi-metric analysis (TGA) was conducted on a TA Instruments TGA Q500 under a nitrogen atmosphere using approximately 7.0 mg of the respective sample by heating from 25 to 500 °C at a rate of 5 °C min^{-1}.

Synthesis of the adamantane modified azo-initiator (azobis-AD)

4,4′-Azobis(4-cyanovaleric acid) (V-501) (0.2 g, 0.71 mmol), Ada-TEG (0.61 g, 1.85 mmol) and DMAP (35 mg, 0.29 mmol) were dissolved in 4 mL of DCM at room temperature. The mixture was cooled to 0 °C in an ice bath and allowed to stir for 15 min. DCC in 1 mL of DCM was added into this mixture dropwise. The mixture was stirred at 0 °C for 30 min, then allowed to warm to room temperature. After stirring for 24 h, the precipitated byproduct was filtered off. The solvent was removed under reduced pressure to obtain a crude product, followed by column purification with ethyl acetate as the eluent (452 mg, 71% yield). ^{1}H NMR (CDCl$_3$) δ (ppm): 4.27 (m, 4H, OCH$_2$CH$_2$OOC), 3.71 (t, 4H, AdOCH$_2$CH$_2$), 3.69–3.63 (m, 16H, OCH$_2$CH$_2$O), 3.67–3.56 (m, 8H, AdOCH$_2$CH$_2$ + OCH$_2$CH$_2$OOC), 2.64–2.32 (m, 8H, COCH$_2$CH$_2$C), 2.13 (s, 6H, Ad[CH$_2$CHCH$_2$]), 1.74 (d, 15H, Ad[CHCH$_2$CH] + CH$_3$), 1.68–1.57 (m, 12H, CHCH$_2$CH[Ad]). ^{13}C NMR (CDCl$_3$) δ (ppm): 171.4, 117.5, 72.3, 72.0, 71.8, 71.3, 70.7, 70.6, 69.0, 64.2, 59.3, 41.5, 36.5, 33.1, 30.6, 29.1, 24.0.

End group modification of polymer coated iron oxide NPs with azobis-AD

Azobis-AD (61 mg, 68 μmol) and Fe$_3$O$_4$@PEG NPs (50 mg) were dispersed in 3 mL of toluene and purged with nitrogen for 20 min. The mixture was stirred in an oil bath at 70 °C for 24 h. End group modified polymer coated MNPs (Fe$_3$O$_4$@PEG@AD) were subsequently purified by dialyzing against acetonitrile using a dialysis membrane (MWCO 3500 Da) for 24 h.

Synthesis of per-(6-deoxy-6-azido)-β-cyclodextrin (β-CD-(N$_3$)$_7$)

β-CD-(N$_3$)$_7$ was prepared according to the previous published report.[27] *Heptakis* (6-deoxy-6-bromo)-β-cyclodextrin (10 g, 6.3 mmol) was dissolved in anhydrous DMF (80 mL) and NaN$_3$ (5.78 g, 88.8 mmol). The resulting suspension was stirred at 70 °C under Ar for 36 h. The suspension was then allowed to cool down and precipitated in 2 L of stirred ice-water. The precipitate was filtered, washed with water and redissolved in DMF (20 mL) and precipitated in 1 L of stirred ice-water. The precipitate was filtered and washed with water and with little acetone. The resulting product was a white solid (yield: 7.2 g, 86.5%) and was dried under vacuum overnight. ^{1}H NMR (400 MHz, DMSO-d_6, 298 K, ppm): δ = 5.90 (d, 7H, 6.8 Hz), 5.75 (d, 7H, 2 Hz), 4.91 (d, 7H, 3.4 Hz), 3.74 (m, 14H), 3.59 (m, 14H), 3.36 (m, 14H, overlap with H$_2$O). MALDI-TOF MS m/z: calculated for C$_{42}$H$_{63}$N$_{21}$O$_{28}$K$^+$: 1348.37; found, 1348.27.

Synthesis of mannose conjugated beta-cyclodextrin (β-CD-(Man)$_7$)

β-CD-(N$_3$)$_7$ (1.96 g, 1.5 mmol) and (2′-propargyl)-beta-D-mannopyranoside (2.61 g, 12 mmol) were dissolved in DMSO

(20 mL) in a Schlenk tube. Bipyridine (0.37 g, 0.0024 mmol) and CuBr (0.17 g, 0.0012 mmol) were added. The resulting mixture was evacuated and filled with argon and 3 freeze–pump–thaw cycles were performed to eliminate oxygen from the reaction mixture. The mixture was then allowed to stir at 50 °C for 24 h. After the reaction, water was added to the reaction medium and the resulting mixture was dialyzed against water. After dialysis, the resulting clear solution was freeze dried.

Synthesis of per-6-deoxy-6-(thiopropyl-2-bromo-2-methyl propanoate)-β-cyclodextrin (β-CD initiator)

Per-6-thio-β-cyclodextrin (2.5 g, 2 mmol), and dithiothreitol (DTT, 618 mg, 4 mmol) were dissolved in 40 mL anhydrous DMF under argon and heated to 60 °C. After 60 h, the reaction mixture was allowed to cool down to room temperature and allyl 2-bromoisobutyrate (14.53 g, 70 mmol) and 2,2-dimethoxy-2-phenylacetophenone (DMPA, 179 mg, 7 mmol) were added to the reaction mixture and stirring was continued for 5 h under UV irradiation (365 nm). The solution was precipitated in 500 mL of methyl *tert*-butyl ether (MTBE) in ten 50 mL centrifuge tubes and centrifuged at 8000 rpm for 5 min. The solvent was decanted and all precipitated fractions collected in two 50 mL centrifuge tubes and fresh MTBE was added, mixed and centrifuged again. This procedure was repeated 4 times in order to remove DMF and allyl 2-bromoisobutyrate. Subsequently the product was dried under vacuum, yielding a fine beige solid. (3.7 g, yield: 68%). ^{1}H NMR (400 MHz, DMSO-d_6, 298 K, ppm): δ = 5.90 (d, 7H, 5.6 Hz), 5.8 (m, 7H), 4.85 (m, 7H), 4.22 (t, 14H, 5.2 Hz), 3.85 (m, 7H), 3.57 (m, 7H), 3.33 (m, 14H), 3.09 (d, 7H, 10.6 Hz), 2.82 (m, 7H), 2.69 (m, 14H), 1.90 (s, 56H). MALDI-TOF MS m/z: calculated for $C_{91}H_{147}Br_7O_{42}S_7K^+$: 2733.12; found: 2733.36.

Synthesis of poly(mannose) conjugated beta-cyclodextrin (β-CD-p(Man)$_{280}$)

A Schlenk tube was charged with the mannose acrylate monomer (580.22 mg, 280 eq.), pre-activated Cu(0) wire (5 cm), CuBr$_2$ (0.35 mg, 0.28 eq.) and Me$_6$TREN (1.70 mg, 1.33 eq.) in DMSO (2 ml) and then the mixture was degassed by gentle bubbling of argon gas for 30 min. The pre-degassed CD initiator in 1 ml DMSO (15 mg, 1 eq.) was then added *via* a gas tight syringe sequentially. The Schlenk tube was sealed and the reaction mixture was allowed to polymerize at 25 °C. Sampling was carried out using a degassed syringe to check the conversion of the monomer. After it reached full conversion, the polymerization solution was directly dialyzed against water for 3 days. The CD initiated glycopolymer was recovered as a powder by freeze drying.

Synthesis of poly(galactose) conjugated beta-cyclodextrin (β-CD-p(Gal)$_{280}$)

β-CD-p(Gal)$_{280}$ was prepared using a similar procedure as above used for β-CD-p(Man)$_{280}$. Details of the procedure and characterization are given in the ESI (Fig. S9†).

Supramolecular complexation between Fe$_3$O$_4$@PEG@AD and β-CD-(Man)$_7$/β-CD-p(Man)$_{280}$

β-CD-(Man)$_7$ or β-CD-p(Man)$_{280}$ was added to 1.67 mg mL^{-1} dispersion of Fe$_3$O$_4$@PEG@AD MNPs in Milli-Q water. The mixture was incubated for 15 min, followed by the collection of MNPs *via* a permanent magnet yielding Fe$_3$O$_4$@PEG@AD/β-CD-(Man)$_7$ and Fe$_3$O$_4$@PEG@AD/β-CD-p(Man)$_{280}$ supramolecular complexes.

Lectin Binding Studies to Mannose Decorated Fe$_3$O$_4$@PEG@AD MNPs. Mannose attached MNPs (1.67 mg mL^{-1}) were mixed with 0.05 mg mL^{-1} FTIC labelled ConA in an aqueous buffer solution (20 mM HEPES, 1.0 mM MnCl$_2$, 1.0 mM CaCl$_2$ and 0.15 M NaCl, adjusted to pH 7.4). The mixture was subjected to a magnet for 10 min to collect MNPs. The fluorescence spectrum of the supernatant was taken at an excitation wavelength of 490 nm.

Selective lectin separation assays

A mixture of lectins (FITC-ConA and rhodamine-PNA) was prepared in a HEPES buffered saline and mannose decorated MNPs (1.67 mg mL^{-1}) were subsequently added to this mixture to selectively capture ConA. The mixture was subjected to a magnet for the separation of lectins. The fluorescence spectrum of the supernatant was recorded at an excitation wavelength for FITC-Con A at 490 nm and Rhd-PNA at 520 nm.

Results and discussion

Polymer coating on MNPs

Iron oxide nanoparticles have been extensively exploited for the magnetic separation and detection of biomolecules.[36–38] Oleic acid stabilized iron oxide nanoparticles (Fe$_3$O$_4$@OA) were synthesized *via* a thermal decomposition method according to the previously reported literature,[20] and characterized by FT-IR (Fig. 2). Asymmetric and symmetric CH$_2$ peaks of oleic acid capped onto the MNP surface appeared at 2916 and 2848 cm^{-1}, respectively (Fig. 3A). The size distribution of Fe$_3$O$_4$@OA NPs was found as an average diameter of 20 nm from DLS analysis (Table 1 and Fig. S3†) and TEM (Fig. 3B–E), revealing spherical particles.

The strategy to grow polymer brushes on the MNP surface begins with immobilization of the RAFT agent (dopa-CTA) on the surface because the catechol unit is known to possess high affinity for a variety of surfaces.[39–41] A place exchange reaction was carried out in the presence of excess dopa-CTA to immobilize the RAFT agent onto the MNP surface.[17] The surface coating of the MNPs with this modified RAFT agent *via* a place exchange reaction was confirmed by FT-IR spectroscopy from the presence of a small band at 1645 cm^{-1} belonging to the amide carbonyl group of dopa-CTA (Fig. 3A). UV-vis spectroscopy also confirmed the presence of the trithiocarbonate based RAFT agent from its characteristic absorption band around 308 nm that was not present in Fe$_3$O$_4$@OA MNPs (Fig. S2†). MNPs did not show any aggregation during the place exchange reaction as indicated in the TEM image of
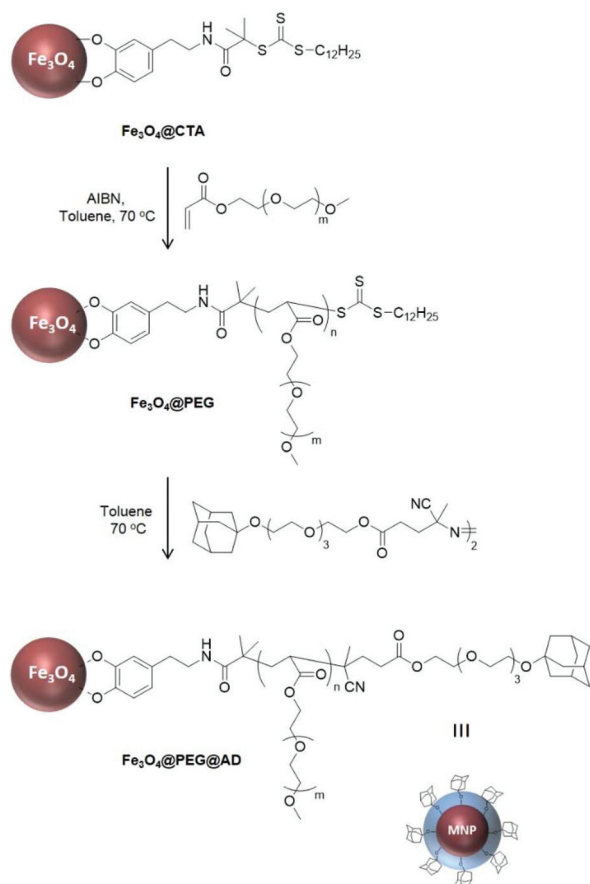
Fig. 2 RAFT polymerization from the MNP surface with the PEGMEA monomer and surface modification of polymer coated NPs with the azobis–ADA initiator.
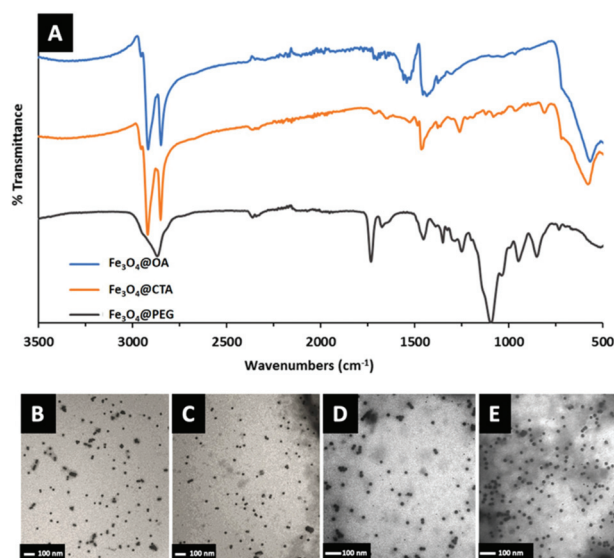

Fig. 3 FT-IR spectrum of Fe$_3$O$_4$@OA, Fe$_3$O$_4$@CTA and Fe$_3$O$_4$@PEG MNPs (A), TEM images of Fe$_3$O$_4$@OA (B), Fe$_3$O$_4$@CTA (C), Fe$_3$O$_4$@PEG (D) and Fe$_3$O$_4$@PEG@AD (E) magnetic nanoparticles.

Table 1 Characteristics of magnetic NPs by DLS, TEM and zeta potential

Samples	D_{DLS} (nm)/PDI	D_{TEM} (nm)	ζ (mV)
Fe$_3$O$_4$@OA	20 (0.46)	19 ± 1.7	—
Fe$_3$O$_4$@CTA	17 (0.47)	19 ± 2.0	—
Fe$_3$O$_4$@PEG	24 (0.46)	19 ± 1.5	−4.5 ± 4.5
Fe$_3$O$_4$@PEG@AD	22 (0.23)	19 ± 2.1	−3.2 ± 4.1

Fe$_3$O$_4$@CTA (Fig. 3C). The hydrodynamic size of the RAFT agent immobilized MNPs was measured as 17 nm from DLS, which was similar to the size of oleic acid coated NPs (Fig. S3†).

The polymer brush coating on the MNP surface was obtained *via* RAFT polymerization with the help of dopa-CTA immobilized onto the surface. The poly(ethylene glycol) methyl ether acrylate (PEGMEA) monomer was used to obtain a dense and hydrophilic anti-biofouling polymer shell on the MNP surface using the "graft-from" approach (Fig. 2). The coating of the hydrophilic PEG polymer on the NP surface was confirmed by FT-IR. The carbonyl stretching of PEG at 1732 cm^{-1} and ether (CH$_2$–O–CH$_2$) stretching at 1093 cm^{-1} were observed from FT-IR analysis, which confirms a successful polymer growth from the surface (Fig. 3A). The hydrodynamic size of Fe$_3$O$_4$@PEG MNPs was determined by DLS measurements, revealing an average diameter of 24 nm. The zeta potential of polymer coated MNPs was measured as −4.5 mV (Table 1). The increase in the hydrodynamic size of the MNPs results from the grafting of a hydrophilic PEG based polymer on the surface. TEM analysis of Fe$_3$O$_4$@PEG NPs revealed that they did not undergo any aggregation during polymerization (Fig. 3D). Furthermore, all these immobilization steps for OA, CTA and PEG polymer respectively on MNPs were confirmed by TGA, as well. As seen in Fig. S12,† the amount of mass loss exhibited an increase after each immobilization step. Each coated MNPs showed mass loss until approximately 450 °C due to the decomposition of the material on it, and the remaining fraction was the Fe$_3$O$_4$ core that was unaffected at high temperature. It was observed that PEG polymer coated MNPs contained 94.5% of the polymer.

Modification of polymer coated MNPs with adamantane

Radical-induced transformation of trithiocarbonate (or thiobenzoate, dithiobenzoate and so on) based end group of the RAFT polymers is a versatile process to obtain desired chain end functionality. Exploiting this methodology, an adamantane group was installed onto the polymer coated nanoparticle surface using the azobis-ADA initiator. The initiator was synthesized from Ada-TEG and 4,4′-azobis(4-cyanovaleric acid) in the presence of DCC and DMAP (Scheme S1†). The structure of the azobis-ADA terminating agent was confirmed using ^{1}H-NMR spectroscopy (Fig. S1†). End group adamantane modified MNPs (Fe$_3$O$_4$@PEG@AD) were synthesized *via* a radical cross-coupling modification reaction at 70 °C with an excess amount of the azobis-ADA initiator (Fig. 2). The modification

of the trithiocarbonate end group of the polymer chain on the MNP surface was monitored by UV-vis spectroscopy. A small absorption shoulder around 308 nm belonging to the trithiocarbonate group disappeared after the cross-coupling modification of the RAFT polymer chain-end on the MNP surface (Fig. S2†). The size distribution of Fe$_3$O$_4$@PEG@AD MNPs obtained from the DLS measurements indicated an average diameter of 22 nm. The zeta potential of adamantane end group modified MNPs was found as −3.2 mV (Table 1). Moreover, the adamantane modified MNPs were characterized by TEM and the presence of discrete MNPs suggested that no aggregation occurred during the radical coupling based end group modification step (Fig. 3).

Synthesis of mannose/galactose-containing beta-CD constructs

Two types of mannose-containing beta-CD constructs were synthesized to tailor the NP interface for effective targeting of the ConA lectin. As depicted in Fig. 4A and B, a β-CD derivative (β-CD-(Man)$_7$) containing seven mannose groups at the lower rim and a star-shaped macromolecular construct (β-CD-p(Man)$_{280}$) containing polymeric arms bearing mannose groups as side chain moieties exuding from the lower rim of CD were synthesized. The β-CD-(Man)$_7$ was synthesized according to a previously reported procedure.[27] Briefly, a beta-CD derivative containing hepta-azide groups at the lower rim was clicked with an alkyne-containing mannose derivative using the copper catalyzed azide–alkyne cycloaddition reaction (CuAAC). As seen in Fig. 4D and E, this successful click reaction was followed by ^{1}H-NMR and DMF GPC analysis. ^{1}H-NMR spectra represented the presence of a new triazole ring peak at approximately 8.0 ppm and also DMF GPC traces showed a significant shift to a lower retention time after the click of mannose alkyne due to the change of hydrodynamic volume.

The polymeric construct that consisted of mannose-containing polymers appended to the bottom rim was synthesized *via* single-electron transfer living radical polymerization (SET-LRP). The homopolymerization of mannose acrylate was carried out using the synthesized beta-CD initiator (β-CD-(Br)$_7$) under high dilution conditions to avoid a radical–radical coupling side reaction according to our previous published report.[42] Briefly, a Schlenk tube was charged with mannose acrylate, preactivated Cu(0) wire, Cu(II)Br$_2$ and Me$_6$Tren in DMSO. The pre-degassed β-CD initiator was then added into the Schlenk tube to start the polymerization at 25 °C. After reaching approximately full conversion according to ^{1}H-NMR, the star-shaped macromolecular construct (β-CD-p(Man)$_{280}$) was obtained in the pure form after dialysis. As seen in Table S1,† GPC analysis using DMF as an eluent showed the increase of M_n to 32 300 g mol^{-1} and polydispersity (Đ) to 1.2 according to poly(styrene) calibration standards, which is still a quite narrow dispersity for such a multiarm star polymer. Moreover, the elution profile revealed a complete shift to a higher molecular weight without any coupling and tailing peaks, strongly indicating a successful synthesis of the polymers (Fig. 4F and G). Furthermore, β-CD-p(Gal)$_{280}$ was synthesized using the same approach to target PNA lectins
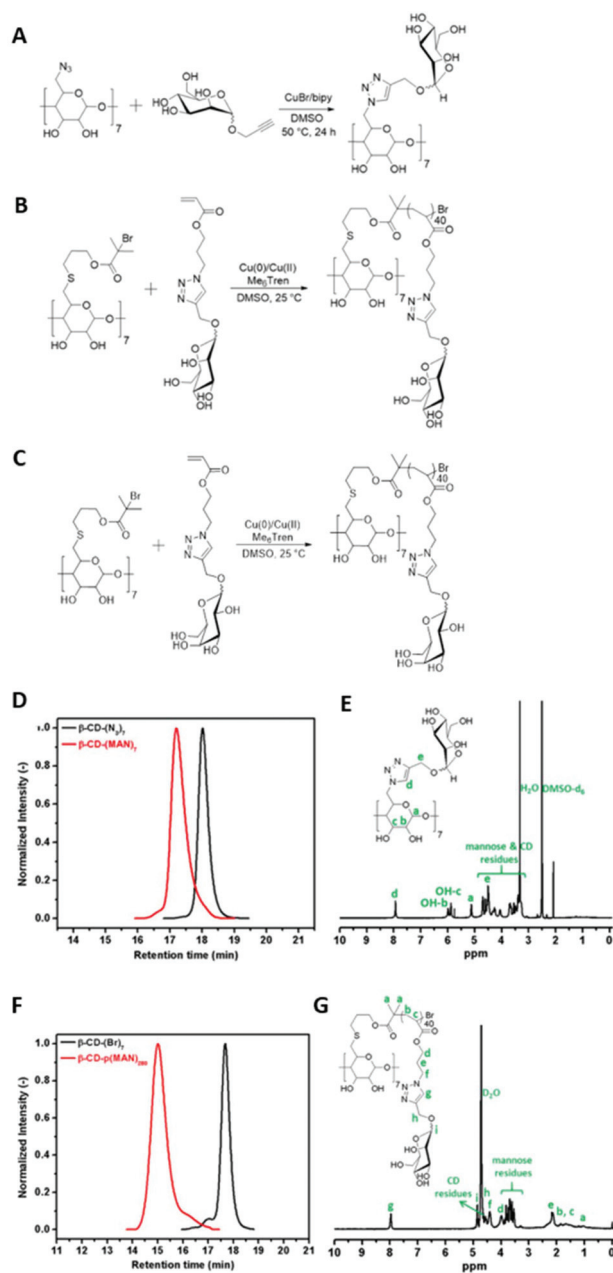

Fig. 4 Synthesis of mannose containing β-CD constructs; β-CD based (mannose)$_7$ (A); β-CD based poly(mannose)$_{280}$ (B); β-CD based poly(galactose)$_{280}$ (C); SEC traces of the synthesized β-CD-(N$_3$)$_7$ and β-CD-(Man)$_7$ (D); ^{1}H NMR spectra of β-CD-(Man)$_7$ (E), SEC traces of the synthesized β-CD-(Br)$_7$ initiator and CD-based mannose glycopolymer (F); ^{1}H NMR spectra of β-CD-p(Man)$_{280}$ (G).

(Fig. 4C), thus demonstrating that binding to a specific protein can be achieved by choosing the appropriate sugar based ligand.

Investigation of host–guest complexation of AD-containing MNPs with mannose appended CD-based constructs

Installation of the adamantane group on the surface of polymer coated magnetic nanoparticles provides them with the ability to undergo non-covalent functionalization through

host–guest interactions with β-cyclodextrins (β-CD). Hence, the ability of the adamantyl moiety on the NP surface to undergo a successful host–guest type complexation with β-CD was examined. A basic phenolphthalein (PP) solution was treated with β-CD and the decrease in absorbance of the dye due to its complexation with the CD cavity was recorded using UV-Vis spectroscopy. Recovery of the absorbance from the dye upon addition of an adamantyl group containing material indicates its complexation with β-CD to liberate the dye from the CD cavity. For the complexation experiments, β-CD (32 μM) was added to a PP solution which is pink in color at pH > 8.2. The decrease in absorbance arising from the inclusion of PP into the β-CD cavity was followed by UV-vis measurements (Fig. 5). The addition of different amounts of Fe_3O_4@PEG@AD MNPs (from 1 to 2 mg) triggered the release of PP from β-CD cavity within a few seconds because adamantane has a higher binding affinity for β-CD compared to PP. A recovery of absorbance ascribed to the release of PP from the cavity was observed upon addition of Fe_3O_4@PEG@AD NPs (Fig. 5). As a control experiment, no recovery of absorbance occurs upon the addition of MNPs devoid of adamantyl groups (1.0 and 1.5 mg). A minimal increase in absorbance was observed upon the addition of more MNPs (2.0 mg), which probably arises from complex formation between the hydrophobic undecane group at the end of polymer brush and β-CD. Background scattering of magnetic NPs in UV analysis did not affect the intensity of the dye because it was found that the UV intensity of PP upon the addition of polymer coated MNPs (from 1 mg to 2 mg) to PP solution showed no intensity increase while MNPs' background scattering was still observable (Fig. S10†). Overall, the results indicated that adamantyl groups were successfully installed onto the polymeric shell on the nanoparticle, and were capable of undergoing specific complexation through host–guest interaction with β-CD.
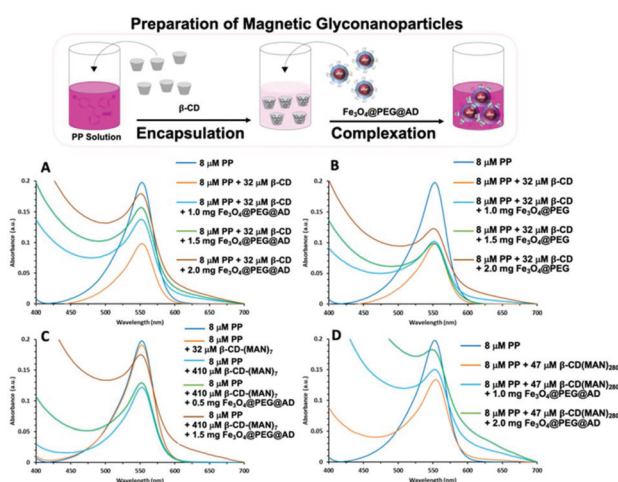

Fig. 5 UV-vis spectra of 8 μM PP solutions at pH = 10.2 with 32 μM β-CD and different amount of Fe_3O_4@PEG@AD MNP addition (A), with 32 μM β-CD and different amount of Fe_3O_4@PEG MNP addition as control experiments (B), with β-CD-(Man)$_7$ (C) and β-CD-p(Man)$_{280}$, followed by mixing with Fe_3O_4@PEG@AD MNPs (D).

After these initial complexation studies, adamantane functionalized MNPs were investigated toward the formation of supramolecular host–guest complexes with the mannose containing β-CD derivatives β-CD-(Man)$_7$ and β-CD-p(Man)$_{280}$. As expected, UV-vis absorbance of the PP solution at 552 nm decreased upon the addition of either β-CD-(Man)$_7$ or β-CD-p(Man)$_{280}$ with increasing concentrations. Fe_3O_4@PEG@AD MNPs were subsequently added to these solutions for complexation with these mannose modified CDs. Recovery of the absorbance in the UV-vis spectra indicated the occurrence of binding between the adamantane groups on the NPs and β-CD derivatives (Fig. 5), thus suggesting that the surface of MNPs could be decorated with these mannose containing CD constructs through host–guest interactions.

Lectin binding to mannose-containing CD-decorated MNPs

First, the MNPs capped with heptamannose were evaluated for binding with fluorescein-containing ConA (FITC-ConA). Fe_3O_4@PEG@AD MNPs were mixed with different concentrations of β-CD-(Man)$_7$ (from 18.7 μM to 800 μM) in Milli-Q water to obtain a Fe_3O_4@PEG@AD/β-CD-(Man)$_7$ complex. Unbound β-CD-(Man)$_7$ was easily removed from the solution by decantation of the supernatant after subjecting the solution to a permanent magnet for 15 min to collect the MNPs. In this manner, surface α-D-mannose decorated Fe_3O_4@PEG@AD/β-CD-(Man)$_7$ MNPs were collected and these MNPs were subsequently used to evaluate Con A binding efficiency. As a control experiment, Fe_3O_4@PEG@AD MNPs were mixed with 410 μM of parent β-CD devoid of mannose groups. These MNPs were also collected using a magnet to obtain the Fe_3O_4@PEG@AD/β-CD inclusion complex. Afterwards, these surface modified MNPs were added to a FITC-ConA containing solution to probe their binding. Fe_3O_4@PEG@AD/β-CD-(Man)$_7$ (1.67 mg mL^{-1}) was added to 0.05 mg mL^{-1} of FITC-ConA solution in HEPES buffered saline (pH 7.4). Binding studies were monitored using fluorescence spectroscopy through excitation of FITC-ConA at 480 nm. After the addition of Fe_3O_4@PEG@AD/β-CD-(Man)$_7$ MNPs (1.67 mg mL^{-1}) to the ConA solution, the MNPs were collected using a magnet (Fig. 6). As expected, a decrease in the fluorescence intensity of the supernatant solution was observed suggesting the binding of ConA to mannose containing MNPs. It was deduced that while Fe_3O_4@PEG@AD MNPs treated with 18.7 μM of β-CD-(Man)$_7$ captured 14.5% ConA from the solution, 50.6% of ConA was captured by MNPs treated with 600 μM of β-CD-(Man)$_7$ based on the decrease in fluorescence intensity of FITC (Fig. 6). The captured lectin amount was determined as 11.2 μg mg^{-1} of Fe_3O_4@PEG@AD/β-CD-(Man)$_7$ MNPs, which was calculated from a calibration curve of FITC-ConA solution (Fig. S11†). It was observed that a saturation was reached where further increase in the concentration of β-CD-(Man)$_7$ from 600 μM to 800 μM did not increase ConA binding (Fig. 6). In a control experiment, no significant fluorescence intensity decrease was observed when the FITC-ConA solution was treated with a similar amount of Fe_3O_4@PEG@AD/β-CD MNPs (1.67 mg mL^{-1}), a construct devoid of any mannose
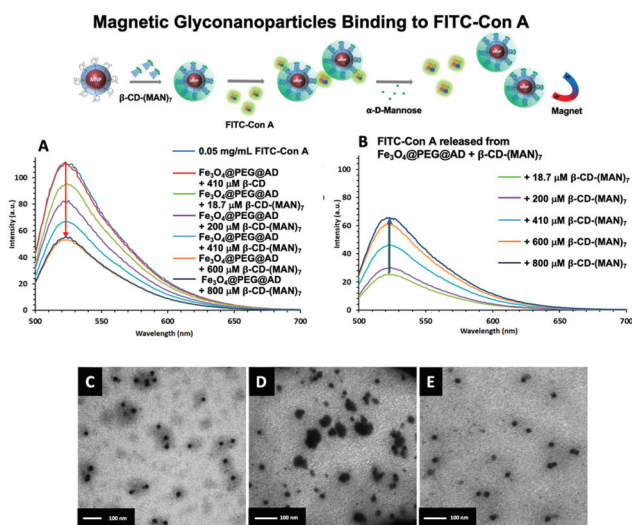
Fig. 6 Host–guest interactions between Fe₃O₄@PEG@AD MNPs and β-CD-(Man)₇, followed by the specific binding of ConA to mannose containing magnetic nanoparticles and release of ConA by the addition of competitive sugar, α-D-mannose; fluorescence spectra of FITC-ConA solution (0.05 mg mL⁻¹) and supernatants from Fe₃O₄@PEG@AD/β-CD-(Man)₇ MNPs containing different amounts of β-CD-(Man)₇ (control experiment was carried out with Fe₃O₄@PEG@AD/β-CD MNPs) (A); fluorescence spectra of ConA release from ConA captured Fe₃O₄@PEG@AD/β-CD-(Man)₇ MNPs upon addition of D-(+)-mannose (B); TEM images of Fe₃O₄@PEG@AD/β-CD-(Man)₇ (C); ConA bound clustered MNPs (D); and redispersed MNPs (E) after the addition of free mannose.

units on the surface of the NPs. These experiments demonstrate that the supramolecular complex of β-CD-(Man)₇ is able to capture ConA from solution.

After the demonstration of the effective capture of ConA from solution, we investigated if they can be released from MNPs. In the presence of high concentrations of a competitive ligand *i.e.* free sugar in the solution, interactions between MNPs and surface bound ConA should diminish leading to the release of bound protein into solution. To this end, the magnetically isolated lectin bound MNPs were redispersed in a HEPES buffered saline and D-(+)-mannose was added to this solution to release captured ConA from MNPs. Upon the addition of sugar, MNPs were separated using a magnet and fluorescence measurements were undertaken on the supernatants to estimate the amount of protein released (Fig. 6). As expected, the highest amount of protein release was observed for 600 μM of β-CD-(Man)₇ immobilized magnetic NPs. The interaction of MNPs with ConA and the subsequent protein release could be followed through TEM analysis (Fig. 6C–E). While the Fe₃O₄@PEG@AD/β-CD-(Man)₇ MNPs were non-aggregated, their treatment with ConA led to the formation of large aggregates due to the bridging interaction between the MNPs and proteins. Furthermore, upon addition of free sugar as a competitive ligand, the complexation between MNPs and ConA was disrupted and discrete MNPs were redispersed in the solution. Although lectin binding using β-CD-(Man)₇ provided an efficient method for the separation of lectins through

multivalent non-covalent interactions, nearly 50% percent of the lectin remained in the solution even upon using a high concentration of the Fe₃O₄@PEG@AD/β-CD-(Man)₇ complex (1.67 mg mL⁻¹). It was observed that an increase in the amount of β-CD-(Man)₇ for the decoration of the MNP surface beyond a certain concentration did not lead to an increase the amount of captured lectin. As an alternative approach, increased concentrations of magnetic NPs can be used, but this strategy is not pragmatic due to the usage of large amounts of magnetic nanoparticles, since apart from cost effectiveness, now more effort will be required to ensure removal of all NPs.

As an alternative, we envisioned that better protein recovery can be achieved and binding efficiency could be perhaps increased using a β-CD-based star glycopolymer since a polymeric construct can be appended with a large number of mannose units for binding to ConA, and the multivalent presentation of ligands on nanoparticle surfaces has been shown to result in increased protein binding.[43] As a first step, β-CD-p(Man)₂₈₀ was immobilized onto the magnetic NP surface *via* host–guest interactions. Surface adamantane decorated MNPs were mixed with different concentrations of β-CD-p(Man)₂₈₀ (from 2 μM to 18.7 μM) in Milli-Q water to obtain the Fe₃O₄@PEG@AD/β-CD-p(Man)₂₈₀ supramolecular inclusion complex. Similar to the first approach, 1.67 mg mL⁻¹ of poly(mannose) containing magnetic NPs were incubated with 0.05 mg mL⁻¹ FITC-ConA solution in HEPES buffered saline at pH 7.4 for 10 min (Fig. 7). After collection of MNPs *via* an external magnetic field, fluorescence spectroscopy measurements were performed for the supernatant. The fluorescence intensity of the FITC labelled ConA dramatically decreased compared to that of the supernatant purified from β-CD-(Man)₇ attached MNPs. MNPs treated with 2 μM of β-CD-p(Man)₂₈₀ were able to collect 26.8% of the lectin while MNPs treated with 18.7 μM of β-CD-p(Man)₂₈₀ captured 86.7% of ConA from the solution that is significantly higher than that of hepta mannose modified β-CD containing NPs (Fig. 7). The lectin capture capacity of poly(mannose) decorated MNPs was determined as 21.8 μg mg⁻¹ of Fe₃O₄@PEG@AD/β-CD-p(Man)₂₈₀ MNPs, using a calibration curve of the FITC-ConA solution. As a control experiment, 1.67 mg mL⁻¹ of the Fe₃O₄@PEG@AD/β-CD MNP dispersion was added to ConA solution and fluorescence spectrum of the supernatant was recorded after the removal of MNPs. As expected, it was deduced that ConA did not interact with these MNPs since there was no decrease in fluorescence intensity.

Recovery of ConA from MNPs was investigated by adding an excess amount of the free sugar D-(+)-mannose as a competitive binder to the protein nanoparticle complex. This resulted in the loss of interaction between ConA and MNPs. MNPs were removed from the solution applying a magnetic field, and the protein content in the supernatant was analyzed using fluorescence spectroscopy. From the measurements, it was deduced that about 83% of ConA captured onto the nanoparticle was released (Fig. 7). Analysis of the protein binding and release process using TEM revealed that discrete
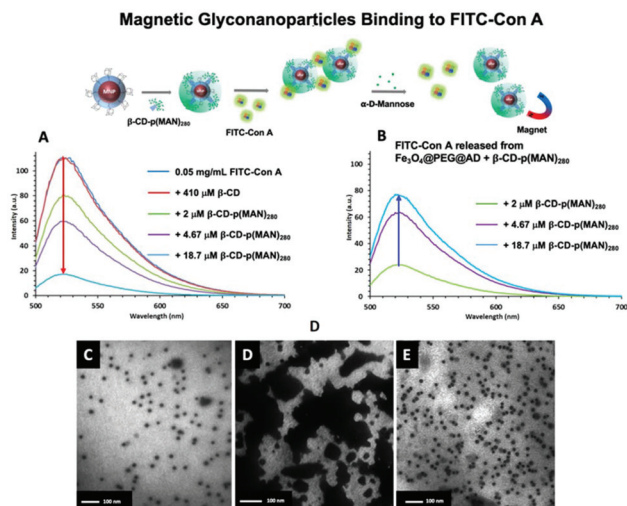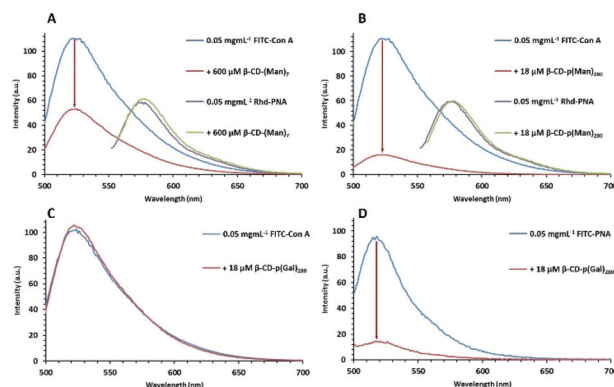
Fig. 7 Host–guest interactions between Fe$_3$O$_4$@PEG@AD MNPs and β-CD-p(Man)$_{280}$, followed by specific binding and subsequent release of ConA. Fluorescence spectra of a FITC-ConA solution (0.05 mg mL^{-1}), and supernatants from Fe$_3$O$_4$@PEG@AD/β-CD-p(Man)$_{280}$ MNPs with different amounts of β-CD-p(Man)$_{280}$ (control experiment was carried out with Fe$_3$O$_4$@PEG@AD/β-CD MNPs) (A); ConA release from MNPs upon the addition of D-(+)-mannose (B) and TEM images of Fe$_3$O$_4$@PEG@AD/β-CD-p(Man)$_{280}$ (C); ConA bound clustered MNPs (D) and redispersed MNPs (E) after the addition of free mannose.

Fig. 8 Fluorescence spectra of supernatants of FITC-ConA, Rhd-PNA and FITC-PNA solutions before and after treatment with: Fe$_3$O$_4$@PEG@AD/β-CD-(Man)$_7$ NPs (A), Fe$_3$O$_4$@PEG@AD/β-CD-(Man)$_{280}$ NPs (B), and Fe$_3$O$_4$@PEG@AD/β-CD-(Gal)$_{280}$ (C) and (D).

Fe$_3$O$_4$@PEG@AD/β-CD-p(Man)$_{280}$ MNPs aggregated into large extended clusters after treatment with ConA (Fig. 7). In general, the clusters formed with the polymeric mannose coated MNPs were larger and extended when compared with the aggregates obtained with the hepta(mannose) coated MNPs. Disintegration of these clusters to release discrete MNPs due to disruption of their interactions with ConA upon the addition of free mannose to the solution was also clearly evident.

Selective lectin binding experiments were carried out using CD-conjugated MNPs with ConA and PNA. ConA selectively binds to mannose while no interactions occur between mannose and PNA. MNPs (1.67 mg mL^{-1}) were separately dispersed in 0.05 mg mL^{-1} of ConA and PNA solutions. ConA bound to mannose containing MNPs whereas PNA did not bind to β-CD-(Man)$_7$ and β-CD-p(Man)$_{280}$ decorated MNPs, as deduced from the fluorescence spectroscopy measurements of the supernatant after the removal of NPs through magnetic separation. The fluorescence intensity of rhodamine-PNA solution (λ_{ext} = 550 nm) did not change, while the fluorescence intensity of ConA decreased significantly (Fig. 8A and B). Specificity towards a particular lectin can be tailored with the appropriate choice of the sugar based ligand. In order to test this, we synthesized a β-CD-based star glycopolymer using a galactose based monomer (see the ESI†). Galactose based ligands are known to have high affinity towards PNA and a lack of affinity for ConA. Using similar procedures as above, MNPs were decorated with β-CD-p(Gal)$_{280}$ to show the selective binding to PNA. A significant decrease in fluorescence of FITC-PNA was observed upon treatment with galactose coated

MNPs (Fig. 8D). As a control experiment, when these nanoparticles were dispersed in FITC-ConA solution and collected with a magnet, no change in fluorescence was observed (Fig. 8C), due to the lack of affinity.

After demonstrating that the engineered MNPs can selectively bind to ConA and they do not show any non-specific binding with PNA, we probed the efficiency of these MNPs for lectin separation from a mixture. A mixture of ConA (0.05 mg mL^{-1}) and PNA (0.05 mg mL^{-1}) was prepared in HEPES buffered saline at pH 7.4 and 1.67 mg mL^{-1} of poly(mannose) decorated MNPs were subsequently added to this solution. MNPs were collected *via* an external magnetic field and fluorescence intensities of supernatants were determined using a fluorescence spectrophotometer. It was deduced that about 86% of ConA in the solution was captured by mannose-containing polymeric CD coated MNPs, based on the decrease in intensity at 518 nm. No non-specific binding of PNA lectin onto MNPs was deduced from no loss of fluorescence intensity at 575 nm (Fig. 9). The ConA bound MNPs were isolated by using a magnet and redispersed in HEPES buffer followed by the addition of 20-fold excess of α-D-mannose. Using this approach, ConA was quantitatively recovered from MNPs as determined by fluorescence measurements. As expected, there was no corresponding fluorescence emission peak suggesting PNA release into the solution during these experiments.

Additional verification of the purity of the captured ConA lectin was performed through MALDI analysis of the protein isolated from the mixture of lectins (Fig. 10). First, it was verified that distinct peaks could be obtained for the two lectins in MALDI analysis. While the peak for ConA was observed at 26.4 kDa, PNA could be observed as a non-overlapping peak at 25.4 kDa. Analysis of the mixture of lectins produced an overlap of the two peaks for individual lectins. Analysis of the ConA recovered from the mixture of the two lectins showed a peak that could be unequivocally assigned to the specific lectin. As a control, PNA was spiked in ConA solutions from 2% to 10% to find out detection limit of PNA in ConA solution. As shown in Fig. 10, even 2% of spiked-PNA was detectable in
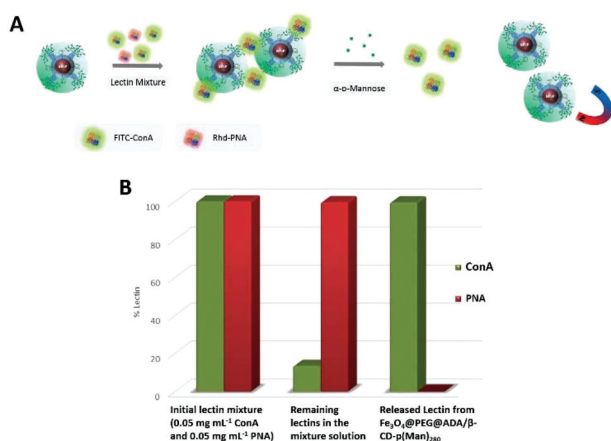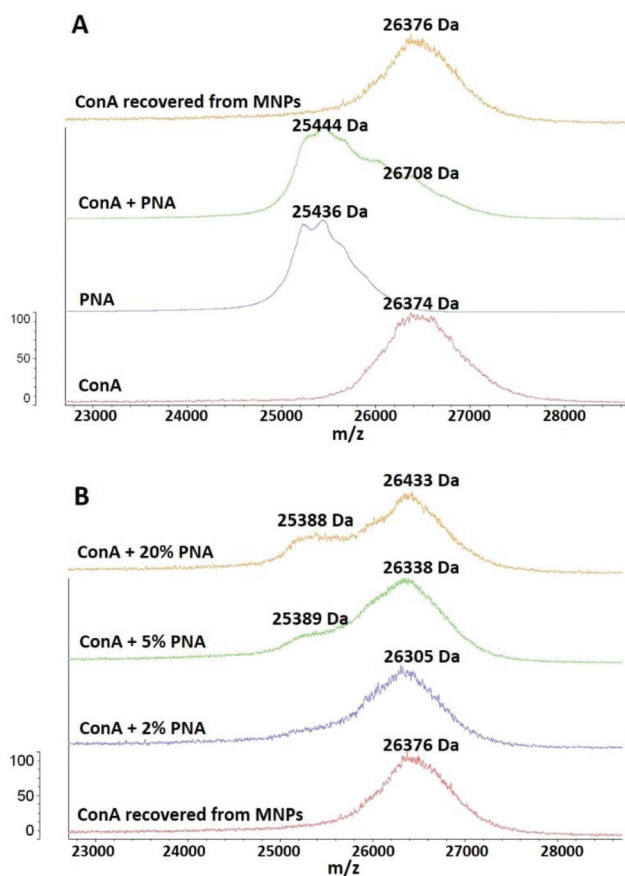
Fig. 9 Illustration of the specific capture of ConA onto Fe$_3$O$_4$@PEG@AD/β-CD-p(Man)$_{280}$ MNPs from a Con A and PNA mixture (A). The release of captured ConA was achieved by the addition of competitive sugar, α-D-mannose; relative amounts of captured lectin from ConA and the PNA mixture with Fe$_3$O$_4$@PEG@AD/β-CD-p(Man)$_{280}$ NPs and recovery of captured lectin upon the addition of α-D-mannose (B).

Fig. 10 MALDI-TOF mass spectra of ConA, PNA, and ConA/PNA mixture (1:1) and recovered ConA from MNPs (A); PNA-spiked ConA solutions in comparison with recovered ConA from MNPs (B).

ConA solution according to the MALDI spectrum. MALDI-TOF mass spectra of isolated ConA from the mixture of lectins indicated that recovered ConA was of high purity with no shoulder peak at 25.4 kDa corresponding to PNA. These results encouraged us to investigate if the lectin of choice can be isolated in the presence of an excess amount of another protein like albumin which is abundant in most biological samples. A mixture of FITC-ConA : BSA (1 : 9) was treated with Fe$_3$O$_4$@PEG@AD/β-CD-p(Man)$_{280}$ NPs. After collection of NPs using a magnet, a decrease of fluorescence intensity due to the depletion of ConA from solution was observed similar to that observed for the ConA solution without BSA (Fig. S13†). This implied that the presence of excess does not interfere with the specific binding to the targeted protein. MALDI analysis of the supernatant solution indicated that all of FITC-ConA was isolated from the solution (Fig. S14†). FITC-ConA bound to the nanoparticle was released by treatment with excess mannose and was analyzed by MALDI to confirm its high purity.

Conclusions

Polymer coated iron oxide nanoparticles appended with adamantane units on the surface allow modular functionalization with sugar containing cyclodextrin based constructs, which provides a modular platform for the separation and purification of lectins. Supramolecular host–guest interactions based on an adamantane beta-cyclodextrin (β-CD) are utilized to modify the polymeric interface. Poly(ethylene glycol) based hydrophilic polymer-coated magnetic iron oxide nanoparticles were fabricated using reversible addition–fragmentation chain transfer polymerization, followed by their chain-end modification to install adamantane groups. Polymer-coated magnetic nanoparticle interfaces bearing adamantane groups were amenable for the modification with mannose-containing β-CD constructs. Two different constructs, monomeric and polymeric mannose conjugated CDs were evaluated for selective binding toward ConA. It was deduced that the polymeric CD construct provided a more effective system separation and purification of ConA from a mixture of ConA and PNA. The surface bound isolated protein could be easily recovered by the addition of mannose, a competitive ligand. Importantly, such selective binding to ConA in a mixture containing excess BSA was also shown. Furthermore, selective binding to PNA is demonstrated using a polygalactose based star glycopolymer. Hence through the appropriate choice of sugar-containing CD-polymers, lectins of choice can be targeted. Thus, it can be envisioned that the nanoparticle interface can be tuned through host–guest chemistry to provide a modular system that can be easily tailored for the purification of specific proteins from mixtures.

Conflicts of interest

There are no conflicts to declare.

Acknowledgements

References

1 C. L. Nilsson, *Anal. Chem.*, 2003, **75**, 348A–353A.

2 P. Bojarová and V. Křen, *Biomater. Sci.*, 2016, **4**, 1142–1160.

3 Z. Yang and W. S. Hancock, *J. Chromatogr. A*, 2004, **1053**, 79–88.

4 Z. Yang and W. S. Hancock, *J. Chromatogr. A*, 2005, **1070**, 57–64.

5 R. Qiu and F. E. Regnier, *Anal. Chem.*, 2005, **77**, 2802–2809.

6 J. Li, Y. Hu, J. Yang, P. Wei, W. Sun, M. Shen, G. Zhang and X. Shi, *Biomaterials*, 2015, **38**, 10–21.

7 S. Sabale, P. Kandesar, V. Jadhav, R. Komorek, R. K. Motkuri and X.-Y. Yu, *Biomater. Sci.*, 2017, **5**, 2212–2225.

8 R. Grifantini, M. Taranta, L. Gherardini, I. Naldi, M. Parri, A. Grandi, A. Giannetti, S. Tombelli, G. Lucarini, L. Ricotti, *et al.*, *J. Controlled Release*, 2018, **280**, 76–86.

9 D. Ling, N. Lee and T. Hyeon, *Acc. Chem. Res.*, 2015, **48**, 1276–1285.

10 M. A. Nash, P. Yager, A. S. Hoffman and P. S. Stayton, *Bioconjugate Chem.*, 2010, **21**, 2197–2204.

11 C. Hu, J. Wu, T. Wei, W. Zhan, Y. Qu, Y. Pan, Q. Yu and H. Chen, *J. Mater. Chem. B*, 2018, **6**, 2198–2203.

12 A. Samanta and B. J. Ravoo, *Angew. Chem., Int. Ed.*, 2014, **53**, 12946–12950.

13 G. Cheng, Z.-G. Wang, Y.-L. Liu, J.-L. Zhang, D.-H. Sun and J.-Z. Ni, *ACS Appl. Mater. Interfaces*, 2013, **5**, 3182–3190.

14 D. T. Ta, R. Vanella and M. A. Nash, *Nano Lett.*, 2017, **17**, 7932–7939.

15 M. Arslan, T. N. Gevrek, J. Lyskawa, S. Szunerits, R. Boukherroub, R. Sanyal, P. Woisel and A. Sanyal, *Macromolecules*, 2014, **47**, 5124–5134.

16 T. Blin, A. Kakinen, E. H. Pilkington, A. Ivask, F. Ding, J. F. Quinn, M. R. Whittaker, P. C. Ke and T. P. Davis, *Polym. Chem.*, 2016, **7**, 1931–1944.

17 K. R. Hurley, H. L. Ring, M. Etheridge, J. Zhang, Z. Gao, Q. Shao, N. D. Klein, V. M. Szlag, C. Chung, T. M. Reineke, *et al.*, *Mol. Pharm.*, 2016, **13**, 2172–2183.

18 C. L. Altan, B. Gurten, R. Sadza, E. Yenigul, N. A. J. M. Sommerdijk and S. Bucak, *J. Magn. Mater.*, 2016, **416**, 366–372.

19 A. Zengin, U. Tamer and T. Caykara, *Biomacromolecules*, 2013, **14**, 3001–3009.

20 Y. Oz, M. Arslan, T. N. Gevrek, R. Sanyal and A. Sanyal, *ACS Appl. Mater. Interfaces*, 2016, **8**, 19813–19826.

21 G. Chen and M. Jiang, *Chem. Soc. Rev.*, 2011, **40**, 2254.

22 J. Willenbacher, B. V. K. J. Schmidt, D. Schulze-Suenninghausen, O. Altintas, B. Luy, G. Delaittre and C. Barner-Kowollik, *Chem. Commun.*, 2014, **50**, 7056.

23 B. V. K. J. Schmidt, M. Hetzer, H. Ritter and C. Barner-Kowollik, *Prog. Polym. Sci.*, 2014, **39**, 235–249.

24 B. V. K. J. Schmidt and C. Barner-Kowollik, *Angew. Chem., Int. Ed.*, 2017, **56**, 8350–8369.

25 X. Ma and Y. Zhao, *Chem. Rev.*, 2015, **115**, 7794–7839.

26 N. Cakir, G. Hizal and C. R. Becer, *Polym. Chem.*, 2015, **6**, 6623–6631.

27 Q. Zhang, L. Su, J. Collins, G. Chen, R. Wallis, D. A. Mitchell, D. M. Haddleton and C. R. Becer, *J. Am. Chem. Soc.*, 2014, **136**, 4325–4332.

28 X. Li, M. Bao, Y. Weng, K. Yang, W. Zhang and G. Chen, *J. Mater. Chem. B*, 2014, **2**, 5569–5575.

29 C. Shao, X. Li, Z. Pei, D. Liu, L. Wang, H. Dong and Y. Pei, *Polym. Chem.*, 2016, **7**, 1337–1344.

30 A. Muñoz-Bonilla, G. Marcelo, C. Casado, F. J. Teran and M. Fernández-García, *J. Polym. Sci., Part A: Polym. Chem.*, 2012, **50**, 5087–5096.

31 J. T. Lai, D. Filla and R. Shea, *Macromolecules*, 2002, **35**, 6754–6756.

32 W. Lv, L. Liu, Y. Luo, X. Wang and Y. Liu, *J. Colloid Interface Sci.*, 2011, **356**(1), 16–23.

33 A. Mulder, S. Onclin, M. Péter, J. P. Hoogenboom, H. Beijleveld, J. ter Maat, M. F. García-Parajó, B. J. Ravoo, J. Huskens, N. F. van Hulst, *et al.*, *Small*, 2005, **1**, 242–253.

34 J. Park, K. An, Y. Hwang, J.-G. Park, H.-J. Noh, J.-Y. Kim, J.-H. Park, N.-M. Hwang and T. Hyeon, *Nat. Mater.*, 2004, **3**, 891–895.

35 Q. Zhang, S. Slavin, M. W. Jones, A. J. Haddleton and D. M. Haddleton, *Polym. Chem.*, 2012, **3**, 1016–1023.

36 H. Gu, K. Xu, C. Xu and B. Xu, *Chem. Commun.*, 2006, 941–949.

37 S. Bucak, D. A. Jones, P. E. Laibinis and T. A. Hatton, *Biotechnol. Prog.*, 2003, **19**, 477–484.

38 Z. Liu, M. Li, X. Yang, M. Yin, J. Ren and X. Qu, *Biomaterials*, 2011, **32**, 4683–4690.

39 Q. Zhang, G. Nurumbetov, A. Simula, C. Zhu, M. Li, P. Wilson, K. Kempe, B. Yang, L. Tao and D. M. Haddleton, *Polym. Chem.*, 2016, **7**, 7002.

40 Y. Oz, A. Barras, R. Sanyal, R. Boukherroub, S. Szunerits and A. Sanyal, *ACS Appl. Mater. Interfaces*, 2017, **9**, 34194–34203.

41 C. E. Brubaker and P. B. Messersmith, *Langmuir*, 2012, **28**, 2200–2205.

42 Y. Abdouni, G. Yilmaz and C. R. Becer, *Macromol. Rapid Commun.*, 2017, **38**, 1700501.

43 S. Boden, K. Wagner, M. Karg and L. Hartmann, *Polymers*, 2017, **9**, 716.